European Journal of Wood and Wood Products
https://doi.org/10.1007/s00107-024-02049-3

ORIGINAL ARTICLE

Hydrophobic and hygroscopic properties of cellulose treated with silicone agents

Waldemar Perdoch[1] · Andreas Treu[2] · Bartłomiej Mazela[1] · Jerzy Majka[1] · Łukasz Czajkowski[1] · Wiesław Olek[1]

Received: 11 October 2023 / Accepted: 17 January 2024

Abstract
The effects of various cellulose treatments on the hydrophobic properties and sorption behavior with respect to liquid water uptake and water vapor sorption were examined within the study. Different hydrophobic agents based on silicon compounds were applied to improve the properties of cellulose-based sheets. The 1H,1H,2H,2H perfluorooctyltriethoxysilane treatment increased hydrophobicity significantly, while N-octyltriethoxysilane and inorganic sodium silicate solution treatments only slightly affected the properties. Silicone-cellulose interaction varied, influencing the fiber saturation and moisture content of the material. The swelling differences between untreated and treated cellulose and, consequently, the uncovering of new active sorption sites during a swelling process and the increase in the content of bound water were confirmed by the T2 relaxation times analysis. The GDW sorption model estimated maximum water content but lacked activation dynamics. The blocking phenomenon of active sorption sites together with silicone improved hydrophobicity had different mechanisms for applied agents. The 1H,1H,2H,2H perfluorooctyltriethoxysilane additionally cross-linked silane structure and restricted cellulose swelling.

1 Introduction

An essential feature of cellulose fibers, resulting from their chemical properties and capillary-porous structure, is their affinity to water (Siau 1984). In industrial applications, this feature is not advantageous. Hydrophilic hydroxyl groups of cellobiose, the fundamental component of cellulose fibers, have a high ability to interact with liquid water and water vapor contained in moist air. The effect of gaining water by cellulose fibers is their swelling, and due to the formed structure containing water bridges, it is also responsible for lower strength properties (Froix and Nelson 1975; Young 1994). In order to reduce these processes, substances should be introduced into the cellulose fibers that will create a steric hindrance effect around the hydroxyl groups, thus limiting or preventing the interaction of water with cellulose or the hydroxyl groups of cellulose. Hydroxyl groups could be substituted with functional groups that do not interact with water molecules, e.g., acetylation or silylation (Kalia et al. 2014; Siuda et al. 2019; Aziz et al. 2022; Rodríguez-Fabià et al. 2022).

In recent years, cellulose coated with silicone compounds, including organosilanes, has been widely used on an industrial scale, including the paper and packaging industry. Silicon compounds are commonly applied for hydrophobic packaging, e.g., packaging dedicated to food or electronics (Kregiel 2014; Bashir et al. 2018; Mazela et al. 2022). However, it should be emphasized that most reports, industrial solutions, and literature data focus on the interaction between liquid water and cellulosic materials (Samyn 2013; Song and Rojas 2013). Only few reports concern water vapor sorption into cellulose or paper. Nowak et al. (2022) and Perdoch et al. (2023) revealed that organosilicon

✉ Waldemar Perdoch
waldemar.perdoch@up.poznan.pl

[1] Faculty of Forestry and Wood Technology, Poznań University of Life Sciences, Wojska Polskiego 28, Poznań 60- 637, Poland

[2] Norwegian Institute of Bioeconomy Research, Høgskoleveien 8, Ås 1433, Norway

compounds modifying starch significantly affected the hydrophobic properties of cellulose sheets and did not change their hygroscopic properties. Camargo and Garcia (2011) studied the adsorption and desorption isotherms as well as sorption hysteresis of composites of regenerated cellulose (cellulose II) and SiO_2. The decrease in hygroscopic properties was found only for one of the tested options, i.e., containing 20% of SiO_2. It was also observed that adding silica promoted the sorption of the primary water compared to the secondary water. Mohammadzadeh et al. (2020) analyzed the hygroscopic properties of cellulose paper treated with commercial products, including hydrophobic and oleophobic agents. Moisture sorption isotherms for untreated and chemically modified paper sheets were investigated and analyzed in the light of the GAB model. The treatment reduced the hygroscopicity and increased the dimensional stability of the paper. Due to the unknown composition of silane in commercial products, it was difficult to discuss the effects of the chemical characteristic on treated materials. The observations may support the phenomenon of the barrier properties for water that organosilicon compounds impart to cellulose fibers. At the same time, the results of the presented analyses (Mohammadzadeh et al. 2020) show that there is no substitution or blocking of active sorption sites in the material, therefore the sorption of water vapor was not limited.

Water vapor sorption significantly affects cellulose fibers (Stevanic and Salmén 2020) and paper (Fellers 2007) properties. Adsorption processes are responsible among others for paper hygroexpansion and its dimensional stability. The strength properties of paper are significantly affected by water vapor sorption, while cyclic changes in the air relative humidity cause mechanosorptive creep. The majority of the literature data concerns cellulose-water interaction through silicone treatments (Qu and He 2013; Ganicz et al. 2020; El-Sabour et al. 2021; Nowak et al. 2022). It is easily recognized that only a few papers presented the cellulose fibers, cellulose pulp, and main products made by cellulose as a topic in the context of both hygroscopic and hydrophobic properties. The increase of the moisture content of a paper product by 1% causes a decrease in the box crush test, i.e. the primary indicator determining the strength of the packaging, by 7–10% (Mark et al. 2002; Frank 2014). Water vapor sorption and its influence on decreased strength can disqualify cellulose in its native form as a material for making ecological products for the catering industry, such as plates and packaging for fast-food products with a high fat or water content. The above-described applications are critical at present, given the strong trends, also sanctioned by the regulations according to the European Union, aiming to eliminate plastics, particularly in single-use products (plates, drinking straws, "food-to-go" packaging). Some of these types of products are already included in the Directive of the European Parliament EU 2019/904 June 5, 2019 on the reduction of the impact of certain plastic products on the environment. Due to the research gap described above, the objective of the present study was to identify and discuss the mechanism responsible for changing the hygroscopic and hydrophobic properties of cellulose protected with selected silicon compounds. The scope of the study included the bulk treatment of cellulose with silicon compounds, producing model paper sheets from cellulose, and then determining silicone retention by the elemental analysis. The most crucial element of the work was the empirical study of the interactions between modified cellulose and water applied in its liquid form and as water vapor in moist air.

2 Materials and methods

2.1 Materials

Bleached softwood Kraft fibers (Södra Black R, commercial form) with the following average dimensions: length − 2100 µm, and width − 30.0 µm were used as the raw material. The fibers were also characterized by the coarseness of 135 µg/m, pH = 4.8, ash content of 0.25%, and brightness of 89.5%. Two types of organosilicon hydrophobic agents, i.e., N-octyltriethoxysilane (NTES) (CAS 2943-75-1, Daw), 1H,1H,2H,2H-Perfluorooctyltriethoxysilane (PFOES) (CAS 51851-37-7, Sigma-Aldrich), and inorganic sodium silicate solution (SiO_2) (CAS 1344-09-8, PPH Standard) were used as hydrophobic agents.

2.2 Cellulose sheets production

Cellulose was firstly immersed in deionized water for 24 h for better defibrillation during cellulose sheets production. A lubricity of diluted suspension of pulp was measured by the Schopper-Riegler apparatus (Labormex, Poland) according to ISO 5267 (2002). The lubricity of the pulp suspension in water in terms of the Schopper-Riegler (SR) number was 14 ± 0.8. The Rapid-Köthen sheet former (Labormex, Poland) was applied to prepare paper sheets with a diameter of 200 ± 0.1 mm and an average thickness of 0.5 ± 0.02 mm. The hydrophobic agents were added during the sheet production according to the compositions presented in Table 1.

2.3 Inductively coupled plasma optical emission spectrometry (ICP-OES) for element analysis

The produced untreated and treated cellulose samples were cut into small particles. Four particles were randomly selected from each tested material and digested

Table 1 Treatment description and their mass ratio

Sample code	Description of treatments	Compositions	Mass ratio between components	Grammage of cellulose (g/m^2)
C	Control	Cellulose	-	308.4 ± 3.2
N	NTES	NTES / cellulose	1:1	304.7 ± 4.3
SiO_2	SiO_2	SiO_2 / cellulose	1:1	305.6 ± 3.5
PF10	PFOES	PFOES / cellulose	1:1	323.6 ± 10.4
PF20	PFOES	PFOES / cellulose	2:1	321.5 ± 5.9
PF40	PFOES	PFOES / cellulose	4:1	310.5 ± 5.1

at the temperature of 240 °C using nitric acid. The iCAP 6000 Series ICP Emission Spectrometer with "dual view of plasma" (Thermo Scientific, USA) was used for the element analysis. The liquid substrates (i.e., NTES and PFOES) were diluted because of the high silicon (Si) concentration. The PFOES was diluted with water and nitric acid in the ratio of 1:100, while the NTES was diluted with ethanol in the ratio of 1:10 and next with water and nitric acid in the ratio of 1:100.

2.4 Low-field nuclear magnetic resonance (LFNMR) analysis

The LFNMR measurements were performed with a mq20 minispec relaxometer with a 0.47 T permanent magnet (Bruker, Billerica, MA, USA). The first set of the samples for the LFNMR analysis was firstly fully saturated with liquid water, and its excess was removed from the sample surfaces with wet cloth. Another set of samples was equilibrated over the saturated salt solutions in order to obtain moisture content levels of ca. 5, 7, and 12% at 40 °C. Such prepared samples were placed in pre-weighed glass tubes and a Teflon rod was inserted to limit water evaporation from the samples. The probe region of the relaxometer was stabilized at 40 °C. The CPMG (Carr-Purcell-Meiboom-Gill) pulse sequence was used to measure the spin-spin relaxation time (T_2) with the pulse separation (τ) of 0.1 ms, 32 000 echoes, gain 73 dB, 16 scans, and a recycle delay of 5 s. The CPMG decay curves were analyzed by the discrete multi-exponential fitting (Pedersen et al. 2002) in MATLAB (MATLAB R2015a, MathWorks, Inc., Natick, MA, USA) and continuous non-negative least squares (NNLS) fitting was applied (Whittall et al. 1991; Lawson and Hanson 1995) using PROSPA 3.2 (Magritek, Aachen, Germany). The NNLS fitting in PROSPA provided continuous distributions of T_2 values. The range for these values was set to 0.9–2600 ms, and 200 data points were determined.

The fiber saturation point (FSP) estimation method was adapted from Telkki et al. (2013). Fully saturated (vacuum method) samples of untreated and treated cellulose were weighed, and then subjected to the LFNMR analysis. After the analysis, the samples were dried to the constant mass (24 h, 103 °C). The decay signal from the LFNMR measurements was transformed into a continuous distribution of exponentials. The integral of a peak in the relaxation time distribution corresponds to the number of nuclei in that environment (Forshult 2004). The peak with the relaxation time T_2 of ca. 100 ms can be attributed to free water, and its area is proportional to free water content in a fully saturated cellulose sample. The difference between the maximum moisture content determined with the gravimetric method and the free water content estimated from the peak area gives the estimated value of the FSP.

2.5 Water contact angle determination

The water contact angle (WCA) measurements were made in order to determine the hydrophobicity of cellulose sheets both untreated and treated with silicon hydrophobic agents. The sessile droplet contact angle was measured with a Kruss contact angle measuring device (Kruss, Germany) at temperature of 20 °C, and air relative humidity of 50%. A water droplet of volume of 1.6 µL was deposited on a sample surface, and a picture of the droplet was taken within 5 s. Then, the pictures were taken every 30 s, and the procedure was repeated ten times. The measurement procedure was repeated five times for each sample.

2.6 Sorption experiments

The studied materials were characterized by low density and relatively high inhomogeneity. Therefore, the sorption experiments were made for sets of samples of dimensions of 0.5 · 50 · 30 mm. The size and number of samples resulted from the error analysis based on the total differential method, e.g. Taylor (1997). Each set of samples corresponded to the individual treatment options of the material. The set-up applied for the sorption experiments consisted of two chambers. The inner chamber was enclosed by the outer one for stabilizing air parameters during the sorption experiments. The salt solutions were used for air relative humidity control in the set-up, and the solutions were successively exchanged during sorption experiments (KNO_3; KCl; NaCl; NaBr; K_2CO_3; $CaCl_2 \cdot 6H_2O$; CH_3COOK; LiCl; P_2O_5). Before placing the samples in the inner chamber with forced airflow and starting the sorption experiments, the procedure of approaching the dry state was applied, i.e. all samples were stored for 3 weeks in closed containers over phosphorus pentoxide. The air temperature during the experiments was equal to 22 ± 1ºC for both adsorption and desorption modes. An electronic thermohygrometer (LB 706, LAB EL,

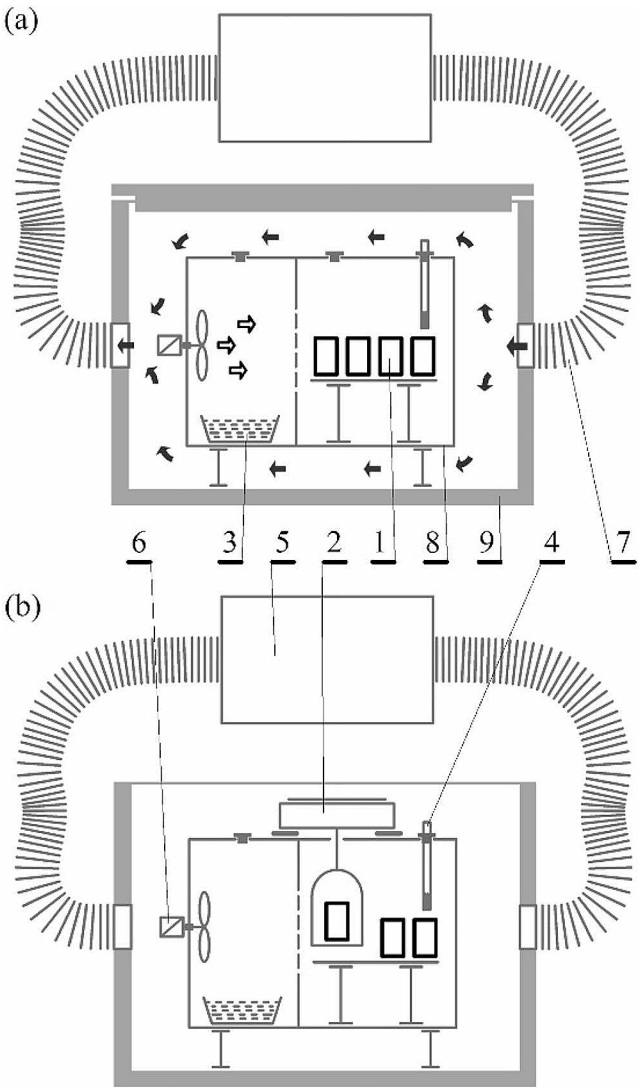

Fig. 1 Scheme of the set-up for sorption experiments: **a** equilibration phase, **b** weighing of equilibrated samples. 1—samples, 2—balance, 3—container with salt solution, 4—thermohygrometer, 5—heat source, 6—fan, 7—ducts of air circulation, 8—inner chamber, 9—outer chamber with thermal insulation)

Table 2 Salt solutions applied in sorption experiments and air relative humidity values at the temperature of 22 ± 1 °C

Salt solution	Relative humidity (–)	
	Adsorption	Desorption
Potassium nitrate (KNO_3)	0.954	0.951
Potassium chloride (KCl)	0.899	0.886
Sodium chloride (NaCl)	0.778	0.791
Sodium bromide (NaBr)	0.600	0.621
Potassium carbonate (K_2CO_3)	0.451	0.463
Calcium chloride ($CaCl_2 \cdot 6H_2O$)	0.324	0.382
Potassium acetate (CH_3COOK)	0.246	0.303
Lithium chloride (LiCl)	0.115	0.116
Phosphorus pentoxide (P_2O_5)	0.041	0.041

Poland) was used to measure the temperature and relative humidity to control the stability of air parameters during the sorption experiments. The samples were weighed at least 5 times at each air relative humidity level. The set-up for the sorption experiments is schematically depicted in Fig. 1. The detailed information on air relative humidity values obtained for the adsorption and desorption modes are given in Table 2, and the values are consistent with data presented by Majka et al. (2023). After finishing the adsorption and desorption modes, all samples were put in a laboratory oven at a temperature of 103ºC to obtain their oven-dry mass. Each equilibrium moisture content value was calculated as the average of 5 observations for each set of samples.

2.7 Sorption isotherms modeling

The sorption isotherms were modeled with two different equations which were separately fitted to all options of untreated and treated cellulose sheets. The Levenberg-Marquardt algorithm implemented in SigmaPlot 9.0 software was used to estimate the best fit of the models.

The three-parameter GAB model was used in the following form, e.g. Timmermann (2003)

$$EMC = M_m \frac{K_{GAB} \cdot C_{GAB} \cdot RH}{(1 - K_{GAB} \cdot RH) \cdot (1 - K_{GAB} \cdot RH + C_{GAB} \cdot K_{GAB} \cdot RH)} \quad (1)$$

where EMC; kg/kg—equilibrium moisture content, RH—air relative humidity, M_m; kg/kg—monolayer capacity, C_{GAB}—equilibrium constant related to the monolayer sorption, K_{GAB}—equilibrium constant related to the multilayer sorption.

The four-parameter GDW equation assumes the existence of the primary sorption sites, which can adsorb only one water molecule, which can be converted into secondary sorption site and/or sites, e.g. Furmaniak et al. (2007). The mathematical structure of the model was

$$EMC = \frac{m_{GAB} \cdot K_{GAB} \cdot RH}{(1 - K_{GAB} \cdot RH)} \cdot \frac{1 - K_{GDW} \cdot (1 - w) \cdot RH}{(1 - K_{GDW} \cdot RH)} \quad (2)$$

where EMC; kg/kg—equilibrium moisture content, RH—air relative humidity, m_{GDW}; kg/kg—monolayer water content (the maximum content of water bound to the primary sites), K_{GDW}—kinetic constant related to sorption on the primary sites, k_{GDW}—kinetic constant related to sorption on the secondary sites, w—ratio of water molecules bound to the primary sites and converted into the secondary sites. The GDW model assumes the following scenarios of the secondary water sorption: (a) $w < 1$—water molecules bound on the primary sites are not completely converted into the secondary sorption sites, (b) $w = 1$—each primary water

molecule is converted into one secondary sorption site, (c) $w > 1$—each primary water molecule is statistically converted into more than one secondary sorption site, and the higher w values are obtained, the more intensive process of water cluster formation occurs.

3 Results

3.1 Element analysis

The concentration of individual elements located in treated and untreated cellulose was used to evaluate the retention of hydrophobic agents in the studied materials (Table 3). The applied bleached softwood Kraft fibers contained significantly higher amounts of Ba, Ca, Mg, Na, S, and Sr as compared to the cellulose treated with silicone hydrophobic agents. Those elements came from a production process of cellulose fibers and were easily leached in the presence of silicone compounds due to changing the chemical environment. In nature, toxic strontium is present mainly in the form of calcium minerals (Capo and Chadwick 1999). The higher strontium concentration in the untreated cellulose and cellulose treated with SiO_2 was directly related to the higher content of calcium compounds. Non-organic silicone additive (SiO_2) increased the concentration of Al, Ca, and Mg in treated cellulose. The most probable reason for the high concentration of those elements was their high concentration in SiO_2 and the influence of silica oxide for agglomeration of the above elements. According to the literature data (Cunha and Gandini 2010; Samyn 2013; Song and Rojas 2013), the critical impact of hydrophobic and hygroscopic properties of paper can be altered by silicones. The silicone concentration in cellulose treated with hydrophobic agents was 3 times higher than in untreated polysaccharides. Independently of the value of the PFOES addition as a hydrophobic agent, the average retention of silicones (silica concentration) was similar and was above 300 mg/kg of the dry mass of treated cellulose. It was found that the silicones in treated cellulose were agglomerated locally, and the concentration was much higher than average (over 1400 mg/kg). The uncertainty of the measurements was less than 10%, with the 95% confidence limit, for values greater than four times of the detection limit. The results for treated and untreated cellulose were given in mg/kg (Table 3), while the results for liquid substances were expressed in mg/L. The element concentration, which was lower than the limit of detection, was presented as a limit of detection (LOD). The silicon concentration in NTES and PFOES were 2640 mg/L and 2060 mg/L, respectively.

3.2 Water-cellulose interaction analyzed by LFNMR

The results of the moisture content of untreated and treated cellulose, as conditioned over the saturated salt solutions prior to the LFNMR analysis, are depicted in Table 4. The untreated samples and samples treated with NTES and SiO_2 were characterized by higher moisture content than those treated with PFOES. These results correspond to the spin-spin relaxation data presented in Fig. 2a. The identification and assignment of the observed peaks within the obtained LFNMR spectra were based on the approach presented by e.g., Felby et al. (2008) and Selig et al. (2013). The peaks observed below 1 ms of the spin-spin relaxation time (T_2) come from bound water. It was found that for cellulose treated with hydrophobic agents, such peaks were identified (Fig. 2a). The T_2 relaxation time in untreated cellulose and cellulose treated with a high concentration of PFOES (PF40) was slightly longer. In both cases, moisture content was higher than 5.5%, and it was a reason that the second weak peak of around T_2 equal to 1 ms was observed. These observations are comparable to the principle described in the literature (Felby et al. 2008) that at the moisture content level of 5%, only bound water is present in cellulose. The weak peak observed for samples with moisture content around 5.5% (Fig. 2a) was much stronger when the moisture content of samples was in a range of 6.5–7.5% (Fig. 2b). The higher intensity of the peaks, around 1 ms, results from the swelling of the cellulose and, consequently, the uncovering of new active sorption sites and the increase in the content of bound water. The slight differences in the intensity of the peaks between the tested materials observed in Fig. 2b most likely indicate a different swelling rate (change in dimensional stability) resulting from the cellulose treatment with silicon-based compounds. A moisture content increase of treated and untreated cellulose by exposing it to moist air over-saturated solution of ammonium phosphate (Table 4) shifts the relaxation time peak to ca. 3 ms (Fig. 2c), which is a characteristic signal that comes from the water contained in the porous fibers of cellulose. In contrast to the observation reported by Felby et al. (2008), there were no two separate peaks characterizing free and bound water, but a broad peak covering signals from two subsystems of bound water. The probable reason of the observed differences in the present study and the data reported by Felby et al. (2008) was the different porosity of treated and untreated cellulose. Chang et al. (2018) analyzed that topic in detail, where the authors described how water transport through the paper is related to the characteristics of the internal pores of the cellulose fibers.

The results of the LFNMR analysis of treated and untreated cellulose, which was fully saturated with liquid water, are presented graphically in Fig. 3. Three

Table 3 Results of ICP-OES element analysis

Sample code	Al	Ba	Ca	Cu	Fe	K	Mg	Na	Pb	S	Si	Sr
	mg/kg											
LOD*	4.0	0.3	18.0	0.6	4.0	33.0	1.0	11.0	0.4	9.0	2.4	0.1
C	5.0	2.8	3011	22.3	9	42	167	303	0.4	135	101	6.8
	4.9	3.4	2966	21.5	9	51	164	297	0.4	125	82	6.7
	4.0	3.0	3019	22.1	9	46	160	309	0.4	135	66	6.7
SiO_2	43.5	1.4	11,121	2.0	24	63	5287	149	0.5	102	594	5.9
	39.5	1.3	11,507	1.7	25	53	5450	141	0.4	102	501	6.0
	36.9	1.4	11,303	2.1	23	59	5289	142	1.1	103	554	5.9
N	5.3	1.1	1054	43.1	17	62	93	117	0.4	101	301	2.8
	5.8	1.1	1085	37.9	19	59	96	127	0.4	104	326	2.8
	4.0	1.2	1080	38.4	20	57	96	133	0.4	104	312	2.8
PF10	4.9	1.1	938	7.0	51	54	82	127	0.5	145	374	2.3
	5.7	1.1	930	6.6	52	51	81	125	0.8	147	1442	2.3
	5.5	1.2	934	6.5	51	43	80	127	0.5	145	370	2.3
PF20	6.8	1.0	735	69.1	42	35	65	109	0.4	129	373	2.0
	7.3	1.3	752	64.3	39	39	66	111	0.6	133	404	2.0
	7.5	1.3	766	65.4	34	39	68	112	0.4	135	673	2.0
PF40	4.3	0.9	708	60.1	30	52	81	113	0.4	149	347	2.0
	4.6	1.0	709	57.0	26	46	83	115	0.5	151	339	2.0
	5.1	1.1	763	62.0	30	46	90	124	0.6	164	1215	2.1

*LOD, limit of detection

Table 4 Moisture content of cellulose samples conditioned over the saturated salt solutions at 40 °C before the LFNMR analysis

Salt solution	Potassium acetate	Magnesium nitrate	Ammonium sulfate
Sample code	%		
C	5.60 ± 0.51	7.57 ± 1.43	13.77 ± 0.85
N	5.43 ± 0.38	6.94 ± 0.67	12.62 ± 0.61
SiO_2	4.29 ± 0.30	7.85 ± 1.05	13.58 ± 2.93
PF10	4.74 ± 1.22	6.58 ± 1.36	11.41 ± 0.62
PF20	4.59 ± 0.47	6.06 ± 0.47	11.25 ± 0.94
PF40	5.65 ± 0.29	7.19 ± 0.68	11.37 ± 0.86

SD, standard deviation; Mean ($n = 3$) ± standard deviation

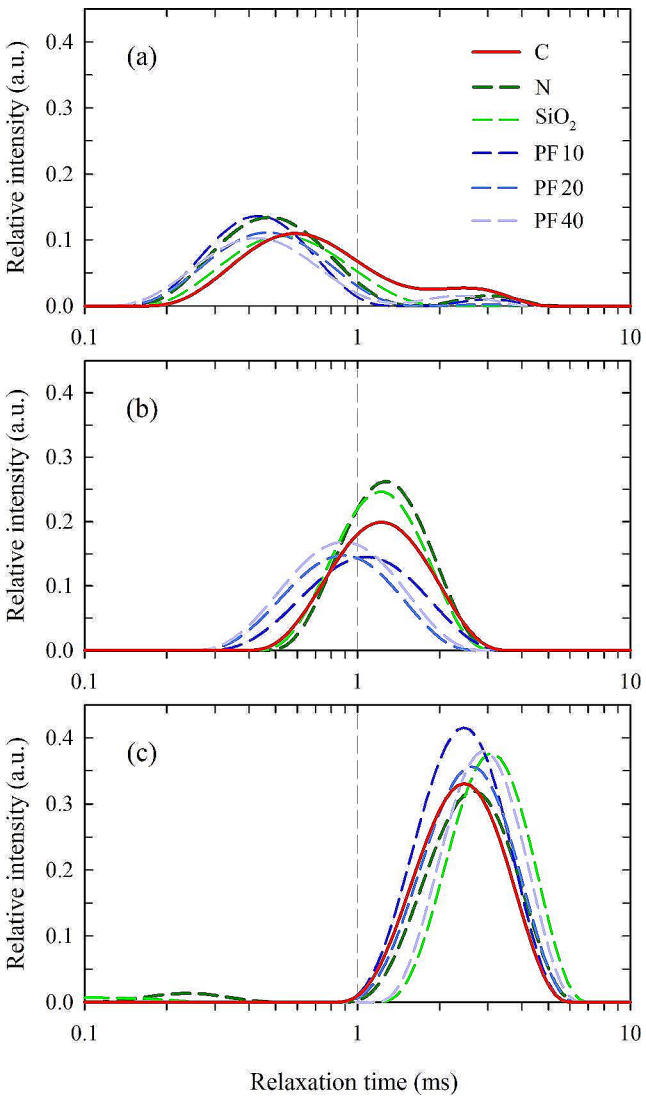

Fig. 2 Time domain of LFNMR of treated and untreated cellulose conditioned above salt solutions: **a** potassium acetate; **b** magnesium nitrate; **c** ammonium sulfate at 40 °C

characteristic peaks can be observed in the regions of 3 ms, 10–30 ms, and 100 ms. The first two peaks can be related to the bound water linked to cellulose, and the last one is free water located between cellulose fibers (Fig. 2). The significantly higher intensity of signals coming from the water subsystem located in the spaces between the fibers can be easily observed. Moreover, the intensity of the peak is significantly reduced due to the applied treatment, e.g. PF 20 (Fig. 4). The calculation of the peak area located around the relaxation time of 100 ms allows for assessing the FSP, by subtracting the free water peak area from the total amount of water. The unmodified cellulose samples (control material) and fully saturated with liquid water were characterized by the moisture content of 280% and the estimated FSP of 40.2 ± 1.6%. The moisture content of the cellulose treated with SiO_2 and NTES and then fully saturated with water was over 300%. In both cases, the calculated FSP significantly exceeded the FSP value found for unmodified cellulose and amounted to 47.2 ± 5.5% and 58.8 ± 1.5%, respectively. The cellulose treatment with PFOES significantly influences the FSP value and reduces water gain. The moisture content of the cellulose samples coded as PF10 was 236 ± 4.0%, and the calculated FSP was 42%. The increase of PFOES concentration during the cellulose treatment resulted in a reduction of the FSP to 25–30% and a reduction of the moisture content of the fully saturated material to ca. 200%. However, no significant differences in silicon concentration in the PFEOS treated cellulose were observed (ICP-OES results, Table 3). The probable reason of the decrease in the FSP was a different cross-linking of the organosilicon hydrophobic agents in the cellulose. The comparison of the maximum moisture content values correlated with the estimated FSP is depicted in Fig. 4.

3.3 Water contact angle analysis

According to literature data (Abdelmouleh et al. 2002; Ganicz and Rozga-Wijas 2021), material surface with a contact angle higher than 90° is recognized as a hydrophobic one. The untreated cellulose samples and samples treated with NTES or SiO_2 did not meet this criterion. Due to the rapid penetration of the water drop into the material, it was impossible to measure the contact angle. Cellulose treated with PFOES, independently of hydrophobic agent concentration, was characterized by very high hydrophobicity. The water contact angle of PF10 samples was 121.3 ± 3.7° and rose after increasing the PFOES concentration and was equal to 133.4 ± 3.1° and 135.9 ± 1.0° for PF20 and PF40, respectively. The results obtained during the contact angle analysis are highly correlated with the results of water gain. The contact angle of untreated cellulose, cellulose treated with SiO_2 or NTES, was not identified due to the fact that a water

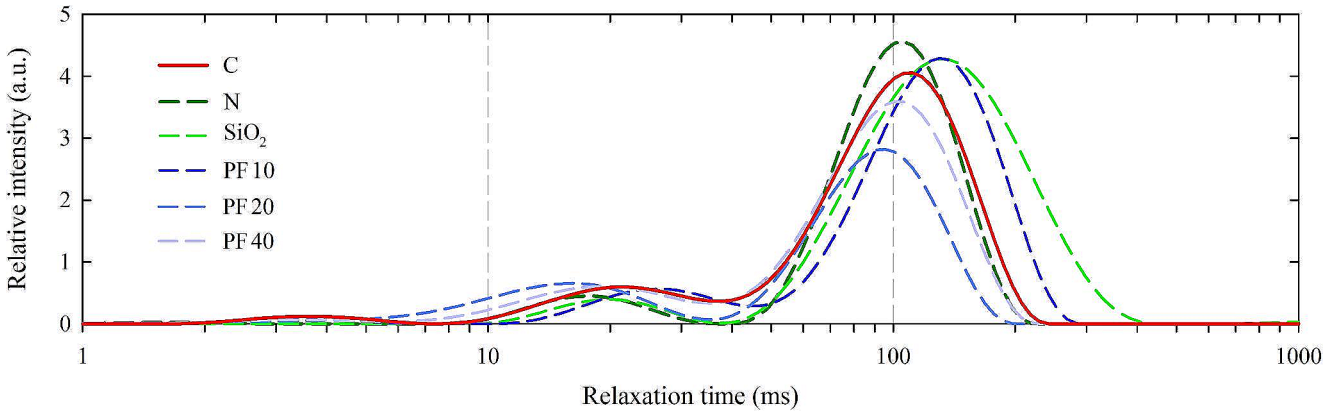

Fig. 3 LFNMR relaxation time of untreated and treated cellulose at the maximum moisture content

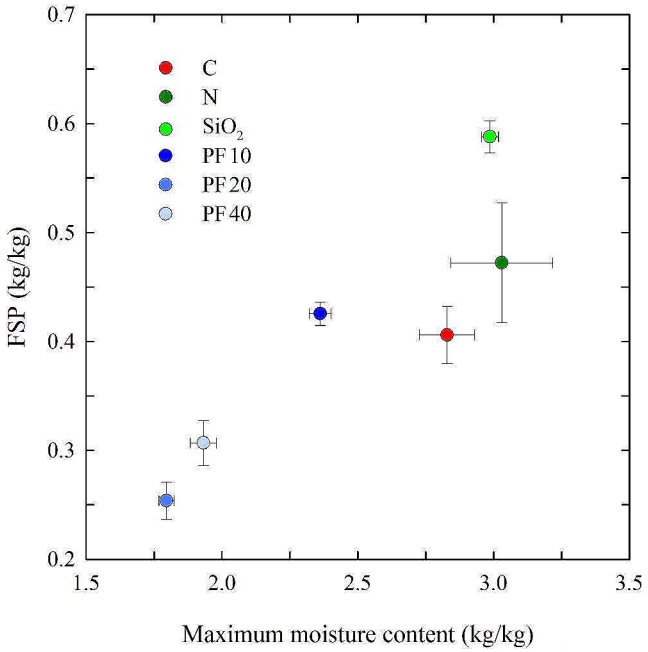

Fig. 4 The maximum moisture content as related to the estimated FSP

drop penetrated a sample immediately after its application. These results correlated with the observations of water gain, i.e., water contact angle was not identified when water gain was higher than 300%. The second group of samples characterized by high contact angle was cellulose treated with PFOES, where water gain was much lower than untreated cellulose and amounted to about 200% for PF20 and PF40 and 250% for PF10. Similar observations on the application of silicone hydrophobic agents with fluorine resulting in superhydrophobic properties of the wood surface, were also presented by Szubert et al. (2019).

3.4 Sorption isotherms analysis

The equilibrium moisture content values measured during the sorption experiments were used to assemble adsorption and desorption isotherms for untreated and treated cellulose sheets. The discrete values of the equilibrium moisture content were plotted together with the predicted values as obtained from the GAB model. The obtained isotherms are depicted in Fig. 5. The applied hydrophobic agents invoked the equilibrium moisture content reduction as compared to the untreated cellulose sheets. However, the improvement of the hygroscopic properties was diversified for the treatment options, i.e. the lowest reduction of the equilibrium moisture content was observed for NTES, while the highest was found for PFOES practically regardless of its concentration.

The results of the GAB model parametrization are presented in Table 5. The fitted values of the monolayer capacity (M_m) were very low and ranged from ca. 0.04 kg/kg to ca. 0.05 kg/kg. It suggests that the majority of absorbed water molecules were linked to the secondary sorption sites. The extremely low values of the monolayer capacity are in contrast with the availability of sorption sites determined with the deuterium exchange method (e.g., Väisänen et al. 2018; Thybring et al. 2021). Therefore, the application of the GAB model seems to be questionable for describing water sorption isotherms of untreated and treated cellulose sheets. The values of the C_{GAB} coefficient are often used to classify sorption isotherm. The values of C_{GAB} fitted in the present study were always higher than 2. Therefore, the necessary condition for ranking the isotherms as type II was satisfied. The C_{GAB} coefficient is related to the sorption enthalpy of the monolayer water and its values were always much higher than K_{GAB}. It suggests that water molecules directly bound to sorption sites are much stronger linked than the secondary water. The values of the K_{GAB} coefficient indicate the difference between the free enthalpy of polymolecular and bulk water (Timmermann 2003). It was

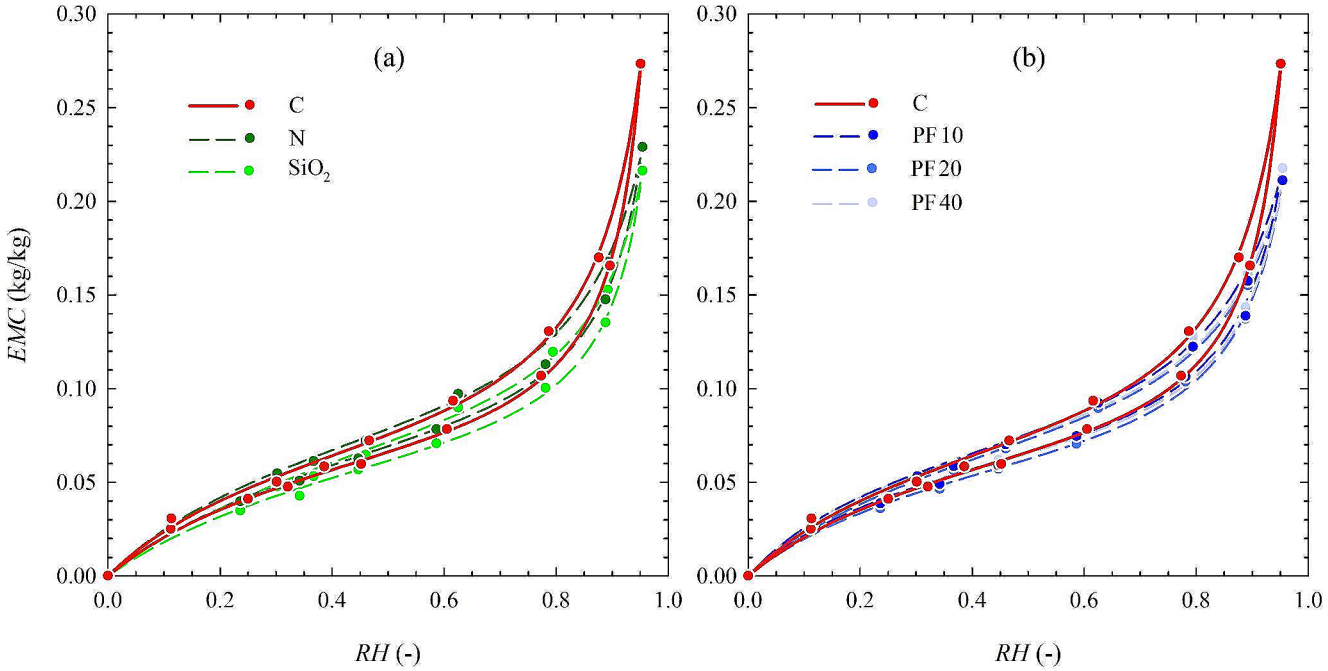

Fig. 5 Adsorption and desorption isotherms of the untreated (Control) and silicone-treated cellulose sheets at temperature of 22 ± 1 °C. The isotherms parametrized with the GDW model, symbols represent experimental data separately measured for each option of the tested materials

Table 5 Estimated coefficients of the GAB model

Sample code	Sorption phase	a	b	c	R^2	M_m (kg/kg)	K_{GAB}	C_{GAB}
C	Adsorption	1.92	22.60	-21.34	0.9339	0.039	0.879	15.419
	Desorption	1.77	19.02	-17.72	0.9590	0.045	0.863	14.491
N	Adsorption	2.06	20.04	-18.15	0.9451	0.043	0.834	13.651
	Desorption	2.04	16.01	-14.11	0.9666	0.052	0.800	11.813
SiO_2	Adsorption	2.20	23.48	-21.57	0.9278	0.037	0.851	14.523
	Desorption	2.12	18.79	-16.82	0.9581	0.045	0.820	12.834
PF10	Adsorption	1.80	22.13	-19.67	0.9557	0.040	0.833	16.794
	Desorption	1.81	17.55	-15.09	0.9707	0.049	0.795	14.212
PF20	Adsorption	2.12	22.67	-20.57	0.9552	0.038	0.841	14.724
	Desorption	2.31	16.91	-14.95	0.9710	0.049	0.797	11.182
PF40	Adsorption	1.89	21.46	-19.21	0.9437	0.041	0.834	15.630
	Desorption	1.85	17.19	-14.94	0.9759	0.050	0.801	13.615

Table 6 Estimated coefficients of the GDW model

Sample code	Sorption phase	m_{GDW} (kg/kg)	K_{GDW}	k_{GDW}	w	R^2
C	Adsorption	0.1026	2.466	0.9906	0.1723	0.9997
	Desorption	0.1043	2.843	0.9576	0.2536	0.9987
N	Adsorption	0.1208	2.029	0.9709	0.1489	0.9987
	Desorption	0.1155	2.631	0.9281	0.2287	0.9992
SiO_2	Adsorption	0.1086	1.967	0.9764	0.1508	0.9984
	Desorption	0.1330	1.761	0.9495	0.1650	0.9977
PF10	Adsorption	0.0945	2.884	0.9597	0.1880	0.9984
	Desorption	0.0937	3.662	0.9137	0.2778	0.9991
PF20	Adsorption	0.0926	2.651	0.9596	0.1998	0.9987
	Desorption	0.1107	2.446	0.9231	0.2313	0.9991
PF40	Adsorption	0.0945	2.918	0.9592	0.1973	0.9990
	Desorption	0.0963	3.484	0.9101	0.2926	0.9986

Table 7 Sorption hysteresis loop (H), the maximum difference of equilibrium moisture content for desorption and adsorption (ΔEMC), and corresponding relative humidity (RH).

Sample code	H (arb. units)	ΔEMC (kg/kg)	RH (™)
C	0.0097	0.018	0.87
N	0.0090	0.017	0.86
SiO_2	0.0087	0.018	0.87
PF10	0.0088	0.017	0.84
PF20	0.0090	0.018	0.85
PF40	0.0092	0.017	0.85

found for untreated material and all options of treatment of cellulose sheets that the K_{GAB} coefficient was always lower than 1. It might suggest that neither the treatment option nor the sorption phase influenced the binding energy of water molecules during polymolecular sorption.

The results of sorption isotherms modeling with the GDW equation are given in Table 6. The predicted maximum content of water bound to the primary sorption sites (m_{GDW}) was equal to ca. 0.1 kg/kg for the adsorption mode. It clearly shows the significance of the primary water sorption as compared to binding water molecules to the secondary sites. The ratio of water molecules bound to the primary sites and converted into the secondary ones (w) was interpreted for the adsorption mode only as it refers to water gain. The w parameter was lower than 0.2 for all analyzed options. It can be deduced that, statistically, less than every fifth molecule of primary water was transformed into the secondary site. The kinetic constant related to sorption on the primary sites (K_{GDW}) was always higher than the kinetic constant referred to sorption on the secondary sites (k_{GDW}). It indicates that water molecules directly sorbed on active sorption sites were more strongly attached to the material than the molecules of secondary water.

The constructed adsorption and desorption isotherms were also used for quantifying sorption hysteresis. The quantification was done with the set of descriptors proposed by Majka et al. (2016). The set comprised a hysteresis loop (H), the maximum difference of equilibrium moisture content for desorption and adsorption (ΔEMC), and corresponding relative humidity (RH). The estimated descriptors of the sorption hysteresis are depicted in Table 7. The applied treatment options had no significant influence on the hysteresis.

The highest value of the air relative humidity applied during the sorption experiments is usually equal to ca. 95%. It signifies that the constructed sorption isotherms cannot be used for estimating the FSP due to unacceptable extrapolation of the equilibrium moisture content values, e.g. Babiak and Kúdela (1995). The statement is also supported by the FSP values estimated in the present study with the LFNMR analysis (Fig. 4), i.e. the FSP values for cellulose treated with NTES or SiO_2 were over 50% and higher than the value for untreated cellulose. Moreover, there was observed reduction of hygroscopic properties in the range of ca. 70–95% air relative humidity (Fig. 5a) for the same treatment options.

4 Conclusion

The identification and explanation of the mechanism responsible for altering hygroscopic and hydrophobic properties of cellulose bulk treatment with silicone hydrophobic agents is ambiguous. The performed analyses on hydrophobic and hygroscopic properties of treated cellulose allowed us to draw the following conclusions:

1. The cellulose treatment with 1H,1H,2H,2H-perfluorooctyltriethoxysilane increased the hydrophobic effect. The water contact angle of the treated material was strongly increased while the fiber saturation point was reduced significantly compared to untreated cellulose. The cellulose treatment with NTES and SiO_2 did not improve the hydrophobic properties. Depending on the applied silicone hydrophobic agents and their concentration, the silicone-cellulose interaction was different. It caused various fiber bulking influencing the observed values of the fiber saturation point and the maximum moisture content.
2. The maximum content of water bound to the primary sites, as estimated by the GDW model, was ca. 0.1 kg/kg. Simultaneously, the ratio of water molecules bound to the primary sites and converted into the secondary ones was usually less than 0.2, i.e., less than every fifth water molecule bound to the primary sorption site was converted into the secondary site. Also, the GDW model does not account for the dynamics of primary sites activation during adsorption. The GDW model describes sorption in a more realistic way as compared to the GAB model. It is primarily due to the fact that the predicted maximum water content bound to the primary sorption sites is estimated by the GAB model, which is very low and inconsistent with the literature results on the availability of sorption sites.
3. The applied silicone hydrophobic agents blocked, to some extent, the active sorption sites resulting in the improvement of the hydrophobic and hygroscopic properties. However, the blocking mechanism and the extent of the improvement were different for the applied agents. The bounding water molecules to the primary sorption sites results in the material swelling, then activating other primary sites. The activation process continues to the saturation (air relative humidity of

100%). The probable mechanism of blocking sorption sites is due to the substituting hydroxyl groups with silicone (Cellulose-O–Si bonds formation). Besides that, applying 1H,1H,2H,2H-perfluorooctyltriethoxysilane is responsible for cross-linking silane structure and restricting cellulose swelling.

Acknowledgements/funding This research was funded by National Center for Research and Development, III edition of EEA and Norway grants; The Program 'Applied Research' in the frame of Norway Grants 2014–2021/POLNOR 2019 (NOR POLNOR/CellMat-4ever/0063/2019-00).

Author contributions Conceptualization, W.P., A.T., B.M., W.O.; Methodology, W.P., A.T., and W.O.; Validation, W.P., A.T., B.M., J.M., Ł.C., and W.O.; Formal Analysis, W.P.; Investigation, W.P., A.T., J.M., and Ł.C.; Writing—Original Draft Preparation, W.P. and W.O.; Writing—Review & Editing, W.P., A.T., B.M., J.M., Ł.C., and W.O.; Supervision, B.M, and W.O.; Project Administration, B.M; Funding Acquisition, B.M.

Funding Open access funding provided by Norwegian Institute of Bioeconomy Research

Data availability Data will be made available on request.

Declarations

Competing interest The authors declare that they have no known competing financial interests or personal relationships that could have appeared to influence the work reported in this paper.

References

Abdelmouleh M, Boufi S, ben Salah A et al (2002) Interaction of silane coupling agents with cellulose. Langmuir 18:3203–3208. https://doi.org/10.1021/la011657g

Aziz T, Farid A, Haq F et al (2022) A review on the modification of cellulose and its applications. Polymers 14:3206. https://doi.org/10.3390/polym14153206

Babiak M, Kúdela J (1995) A contribution to the definition of the fiber saturation point. Wood Sci Technol 29:217–226. https://doi.org/10.1007/BF00204589

Bashir A, Jabeen S, Gull N et al (2018) Co-concentration effect of silane with natural extract on biodegradable polymeric films for food packaging. Int J Biol Macromol 106:351–359. https://doi.org/10.1016/j.ijbiomac.2017.08.025

Camargo JR, Garcia CAO (2011) Effect of silicification on the water sorption properties of microcrystalline cellulose II. Brazilian J Pharm Sci 47:125–135. https://doi.org/10.1590/S1984-82502011000100016

Capo RC, Chadwick OA (1999) Sources of strontium and calcium in desert soil and calcrete. Earth Planet Sci Lett 170:61–72. https://doi.org/10.1016/S0012-821X(99)00090-4

Chang S, Seo J, Hong S et al (2018) Dynamics of liquid imbibition through paper with intra-fibre pores. J Fluid Mech 845:36–50. https://doi.org/10.1017/jfm.2018.235

Cunha AG, Gandini A (2010) Turning polysaccharides into hydrophobic materials: a critical review. Part 1. Cellulose Cellulose 17:875–889. https://doi.org/10.1007/s10570-010-9434-6

El-Sabour MA, Mohamed AL, El-Meligy MG, Al-Shemy MT (2021) Characterization of recycled waste papers treated with starch/organophosphorus-silane biocomposite flame retardant. Nord Pulp Pap Res J 36:108–124. https://doi.org/10.1515/npprj-2020-0075

Felby C, Thygesen LG, Kristensen JB et al (2008) Cellulose–water interactions during enzymatic hydrolysis as studied by time domain NMR. Cellulose 15:703–710. https://doi.org/10.1007/s10570-008-9222-8

Fellers C (2007) The interaction of paper with water vapour. Paper Products–Physics and Technology 109–144

Forshult SE (2004) Quantitative analysis with pulsed NMR and the CONTIN computer program. Report. Karlstad: Department of Physical Chemistry, Karlstad University

Frank B (2014) Corrugated box compression—A literature survey. Packaging Technol Sci 27:105–128. https://doi.org/10.1002/pts.2019

Froix MF, Nelson R (1975) The interaction of water with cellulose from nuclear magnetic resonance relaxation times. Macromolecules 8:726–730. https://doi.org/10.1021/ma60048a011

Furmaniak S, Terzyk AP, Gauden PA (2007) The general mechanism of water sorption on foodstuffs–importance of the multitemperature fitting of data and the hierarchy of models. J Food Eng 82:528–535. https://doi.org/10.1016/j.jfoodeng.2007.03.012

Ganicz T, Rozga-Wijas K (2021) Siloxane-starch-based hydrophobic coating for multiple recyclable cellulosic materials. Materials 14:4977. https://doi.org/10.3390/ma14174977

Ganicz T, Olejnik K, Rózga-Wijas K, Kurjata J (2020) New Method of Paper Hydrophobization based on starch-cellulose-siloxane interactions. BioResources 15:4124–4142. https://doi.org/10.15376/biores.15.2.4124-4142

Kalia S, Boufi S, Celli A, Kango S (2014) Nanofibrillated cellulose: surface modification and potential applications. Colloid Polym Sci 292:5–31. https://doi.org/10.1007/s00396-013-3112-9

Kregiel D (2014) Advances in biofilm control for food and beverage industry using organo-silane technology: a review. Food Control 40:32–40. https://doi.org/10.1016/j.foodcont.2013.11.014

Lawson CL, Hanson R (1995) Linear least squares with linear inequality constraints, solving least squares problems. Society for Industrial and Applied Mathematics, pp 158–173

Majka J, Czajkowski Ł, Olek W (2016) Effects of cyclic changes in relative humidity on the sorption hysteresis of thermally modified spruce wood. BioResources 11:5265–5275. https://doi.org/10.15376/biores.11.2.5265-5275

Majka J, Perdoch W, Czajkowski Ł, Mazela B, Olek W (2023) Sorption properties of paper treated with silane-modified starch. Eur J Wood Prod 81:1581–1590. https://doi.org/10.1007/s00107-023-01976-x

Mark RE, Habeger CC, Borch J, Lyne MB (2002) Handbook of physical testing of paper. CRC Press, Boca Raton

Mazela B, Tomkowiak K, Jones D (2022) Strength and moisture-related properties of filter paper coated with nanocellulose. Coatings 12:1376. https://doi.org/10.3390/coatings12101376

Mohammadzadeh A, Barletta M, Gisario A (2020) Manufacturing of cellulose-based paper: dynamic water absorption before and after fiber modifications with hydrophobic agents. Appl Phys A 126:383. https://doi.org/10.1007/s00339-020-03577-4

Nowak T, Mazela B, Olejnik K et al (2022) Starch-silane structure and its influence on the Hydrophobic properties of Paper. Molecules 27:3136. https://doi.org/10.3390/molecules27103136

Pedersen HT, Bro R, Engelsen SB (2002) Towards rapid and unique curve resolution of low-field NMR relaxation data: Trilinear SLICING versus two-dimensional curve fitting. J Magn Reson 157:141–155. https://doi.org/10.1006/jmre.2002.2570

Perdoch W, Mazela B, Tavakoli M, Treu A (2023) High hydrophobic silanized paper: material characterization and its biodegradation through brown rot fungus. Waste Manag 160:165–172. https://doi.org/10.1016/j.wasman.2023.02.007

Qu J, He L (2013) Synthesis and properties of silane-fluoroacrylate grafted starch. Carbohydr Polym 98:1056–1064. https://doi.org/10.1016/j.carbpol.2013.07.015

Rodríguez-Fabià S, Torstensen J, Johansson L, Syverud K (2022) Hydrophobization of lignocellulosic materials part II: chemical modification. Cellulose 29:8957–8995. https://doi.org/10.1007/s10570-022-04824-y

Samyn P (2013) Wetting and hydrophobic modification of cellulose surfaces for paper applications. J Mater Sci 48:6455–6498. https://doi.org/10.1007/s10853-013-7519-y

Selig MJ, Thygesen LG, Johnson DK, Himmel ME, Felby C, Mittal A (2013) Hydration and saccharification of cellulose Iβ, II and III I at increasing dry solids loadings. Biotechnol Lett 35:1599–1607. https://doi.org/10.1007/s10529-013-1258-7

Siau JF (1984) Permeability. Transport processes in wood. Springer Series in Wood Science, Springer, Berlin, Heidelberg. p 73–104.

EN ISO 5267-1/AC:2002 Pulps - Determination of drainability - Part 1: Schopper-Riegler method

Siuda J, Perdoch W, Mazela B, Zborowska M (2019) Catalyzed Reaction of Cellulose and Lignin with Methyltrimethoxysilane—FT-IR, 13 C NMR and 29Si NMR Studies. Materials 12(2006). https://doi.org/10.3390/ma12122006

Song J, Rojas OJ (2013) Paper chemistry: approaching super-hydrophobicity from cellulosic materials: a review. Nord Pulp Pap Res J 28:216–238. https://doi.org/10.3183/npprj-2013-28-02-p216-238

Stevanic JS, Salmén L (2020) Molecular origin of mechano-sorptive creep in cellulosic fibres. Carbohydr Polym 230:115615. https://doi.org/10.1016/j.carbpol.2019.115615

Szubert K, Dutkiewicz A, Dutkiewicz M, Maciejewski H (2019) Wood protective coatings based on fluorocarbosilane. Cellulose 26:9853–9861. https://doi.org/10.1007/s10570-019-02737-x

Taylor JR (1997) Error analysis, vol 20. Univ Science Books, Sausalito, California

Telkki V-V, Yliniemi M, Jokisaari J (2013) Moisture in softwoods: fiber saturation point, hydroxyl site content, and the amount of micropores as determined from NMR relaxation time distributions. Holzforschung 67:291–300. https://doi.org/10.1515/hf-2012-0057

Thybring EE, Boardman CR, Zelinka SL, Glass SV (2021) Common sorption isotherm models are not physically valid for water in wood. Colloids Surf a 627:127214. https://doi.org/10.1016/j.colsurfa.2021.127214

Timmermann EO (2003) Multilayer sorption parameters: BET or GAB values? Colloids and surfaces. Physicochemical and Engineering Aspects 220:235–260. https://doi.org/10.1016/S0927-7757(03)00059-1

Väisänen S, Pönni R, Hämäläinen A, Vuorinen T (2018) Quantification of accessible hydroxyl groups in cellulosic pulps by dynamic vapor sorption with deuterium exchange. Cellulose 25:6923–6934. https://doi.org/10.1007/s10570-018-2064-0

Whittall KP, Bronskill MJ, Henkelman RM (1991) Investigation of analysis techniques for complicated NMR relaxation data. J Magn Reson (1969) 95:221–234. https://doi.org/10.1016/0022-2364(91)90213-D

Young RA (1994) Comparison of the properties of chemical cellulose pulps. Cellulose 1:107–130. https://doi.org/10.1007/BF00819662